

## **UC Davis**

### **Recent Work**

#### **Title**

Smart Parking Pilot on the Coaster Commuter Rail Line in San Diego, California

#### **Permalink**

<https://escholarship.org/uc/item/5m51w2ns>

#### **Authors**

Blake, Tagan  
Rodier, Caroline J.  
Shaheen, Susan

#### **Publication Date**

2008

Peer reviewed

## Accepted Manuscript

Title: Optimization of Fuel Cell System Operating Conditions for Fuel Cell Vehicles

Authors: Hengbing Zhao, Andrew F. Burke

PII: S0378-7753(08)01929-0  
DOI: doi:10.1016/j.jpowsour.2008.10.032  
Reference: POWER 11219

To appear in: *Journal of Power Sources*

Received date: 18-9-2008  
Accepted date: 3-10-2008

Please cite this article as: H. Zhao, A.F. Burke, Optimization of Fuel Cell System Operating Conditions for Fuel Cell Vehicles, *Journal of Power Sources* (2008), doi:10.1016/j.jpowsour.2008.10.032

This is a PDF file of an unedited manuscript that has been accepted for publication. As a service to our customers we are providing this early version of the manuscript. The manuscript will undergo copyediting, typesetting, and review of the resulting proof before it is published in its final form. Please note that during the production process errors may be discovered which could affect the content, and all legal disclaimers that apply to the journal pertain.



# Optimization of Fuel Cell System Operating Conditions for Fuel Cell Vehicles

Hengbing Zhao\* and Andrew F. Burke

Institute of Transportation Studies, University of California, Davis CA 95616 USA

## Abstract

Proton Exchange Membrane fuel cell (PEMFC) technology for use in fuel cell vehicles and other applications has been intensively developed in recent decades. Besides the fuel cell stack, air and fuel control and thermal and water management are major challenges in the development of the fuel cell for vehicle applications. The air supply system can have a major impact on overall system efficiency. In this paper a fuel cell system model for optimizing system operating conditions was developed which includes the transient dynamics of the air system with varying back pressure. Compared to the conventional fixed back pressure operation, the optimal operation discussed in this paper can achieve higher system efficiency over the full load range. Finally, the model is applied as part of a dynamic forward-looking vehicle model of a load-following direct hydrogen fuel cell vehicle to explore the energy economy optimization potential of fuel cell vehicles.

**Keywords:** fuel cell system; direct hydrogen fuel cell vehicle; optimization model; simulation

\*Corresponding author. Tel.: +1 (530) 754-9000; fax: +1 (530) 752-6572.  
E-mail addresses: [hbzhao@ucdavis.edu](mailto:hbzhao@ucdavis.edu) (H. Zhao),  
[afburke@ucdavis.edu](mailto:afburke@ucdavis.edu) (A.F. Burke).

## 1 Introduction

In recent decades the hydrogen Proton Exchange Membrane fuel cell (PEMFC) technology for use in fuel cell vehicles has been intensively developed by major auto companies. However, the use of fuel cells in vehicles is still far from the mass production subject to further technical development such as durability and cost [1]. Fuel cell applications in automobiles are particularly difficult because of the rapidly varying driving conditions in these applications. The fuel cell system consisting of the stack, air and fuel subsystem and water and thermal management subsystem is often designed to achieve a specified maximum power and the operation is optimized around the nominal operating point in order to maximize the overall system efficiency. In automotive applications, the fuel cell systems have to be able to adapt to a wide range of operating conditions such as frequent start-up and stop, sudden load changes, and varying power levels. Improper system design and control can cause air/fuel starvation, flooding, membrane drying, and pressure imbalance across the membrane, which will damage the fuel cell stack. Therefore, there is a need to develop a tool to optimize the fuel cell system operation over the full load range to achieve stable system operation and maximum fuel economy.

Much work has been done in the past to model fuel cell systems, optimize the operating conditions, and simulate the fuel cell vehicles. Fuel cell models at the cell level are presented in [2-4]. Studies concerned with optimum operating conditions are discussed in [5-12]. The characteristics of the low pressure and high pressure fuel cell systems are addressed with regard to the system efficiency and transient response in [7,13,14].

Lumped filling/emptying dynamic fuel cell models are presented in [15-17]. Air supply control strategies and analyses based on dynamic quasi-steady fuel cell operation are described in [15,18-23]. These studies established a good foundation for understanding fuel cell systems and fuel cell vehicles. However, the above models were developed for a specific fuel cell system or without considering the design of the stack, sizing of the system, or optimization of operating conditions. In addition, the models did not treat the transient dynamics of the system and its effect on system efficiency. A fuel cell system optimization model which treats on a controls basis the transient dynamics of the system and is applicable to a generic fuel cell design (scalable to fuel cells of arbitrary power) is needed for evaluating the fuel cell system in vehicles of various classes and for exploring the energy economy of those vehicles. The development and application of such a model are the subjects of this paper.

The fuel cell system and its integration into a fuel cell vehicle are presented in section 2. The quasi-steady optimization model and optimum highest efficiency operation including transient dynamic effects are described in section 3. Simulation results of fuel cell-powered vehicles with optimum operating conditions on various driving cycles are presented in section 4. The conclusions are summarized in section 5.

## **2 Fuel Cell System for Vehicles**

### ***2.1 Fuel Cell System***

The fuel cell stack is the heart of a fuel cell system. However, without auxiliary components such as the air compressor, humidifier and pressure and flow regulators, the

stack itself would not work. Fuel cell system configurations vary considerably in different applications. A direct hydrogen fuel cell system, as shown in Fig.1, typically involves the following four major auxiliary subsystems: air supply and control, fuel supply and control, water management, and thermal management subsystems. The air supply subsystem includes interacting components, namely, air compressor and expander, supply manifold, cathode side of the fuel cell stack, return manifold, and back pressure control valve. The fuel supply subsystem consists of a high pressure fuel tank, pressure regulator, supply manifold, the anode side of the fuel cell stack, and purge control valve. Water management subsystem includes air/fuel humidifiers or vapor injector and vapor condenser. The thermal management consists of the cooling loop for the stack and temperature control for humidifiers and a radiator. The four subsystems interact and have a large effect on the performance and efficiency of the fuel cell stack.

The fuel cell system operation is complex due to the coupling of the subsystems - the stack, air and fuel supply, and the water and thermal management. In modeling the system, care must be taken to include the level of model complexity needed to adequately account for the impact of the different components on the overall system. The effect of transient phenomena on the electrochemical processes in the stack can be ignored due to their fast response. The response of the water and thermal management subsystems is relatively slow. Hence, the stack and humidifier temperature change slowly and can be considered as constants. Compared to the air filling/emptying dynamics, hydrogen supply from a high pressure tank is fast and its dynamics can be ignored. Therefore, only the transient dynamics related to the air supply subsystem can have a large impact on the

system performance and it is considered in the model. The parasitic loss from the air supply system accounts for about 80 percent of the total losses. Therefore, the air supply has a dominant impact on the system efficiency. The parasitic the losses from the water and thermal management subsystems used in the optimization model are scaled from the quasi-steady model [6] of those systems.

A dynamic air supply model including the fuel cell stack manifold and channels and the compressor was developed and then integrated into the fuel cell system/vehicle model developed by the UCD fuel cell vehicle modeling group [5,11,21]. The system shown in Fig.2 contains component models for each of the key fuel cell system components.

The stack current is used to calculate the hydrogen required. The optimum operating conditions such as mass flow, back pressure, and water and thermal management data, obtained from the quasi-steady fuel cell system optimization model, are used in the dynamic model. The optimal air mass flow is achieved through a combination of feed-back and feed-forward control of the compressor. The back pressure of the stack is controlled by adjusting the opening area of the throttle through a feed-back and feed-forward controller. Therefore, the fuel cell system is controlled to operate around its optimum conditions. The details of the transient dynamic model are given in [24].

## **2.2 Fuel Cell Vehicle Model**

The dynamic fuel cell system model was integrated into a forward-looking vehicle model of a load-following direct hydrogen fuel cell vehicle (DHFC). The fuel cell vehicle was not hybridized with a battery. The driver end of the fuel cell vehicle model shown in

Fig.3 consists of three main blocks: drive cycle, driver, and vehicle. The detailed vehicle model can be seen in [21,22]. The block of drive cycle defines the driving profile as velocity vs. time. The driver block represents the driver properties, generating the acceleration and brake commands to the vehicle block according to the driving cycle and the actual vehicle velocity. The block of vehicle includes vehicle body, traction motor and transmission, and fuel cell system. The motor and transmission subroutines generate the fuel cell current command for the fuel cell system model. Simulations are performed for various drive cycles such as FUDS, US06, HIWAY, JP1015, ECE, and NEDC.

In a fuel cell vehicle, the hydrogen fuel may not be fully utilized. For closed end hydrogen fuel cell systems, frequent purging is used to remove the accumulated water vapor and nitrogen diffused through the membrane. The purging parasitic loss is neglected in this model. For an open-end hydrogen fuel cell, a pump is employed to circulate the unused hydrogen. This loss can be significant, but compared to the air supply system and cooling system, the power consumption of the fuel supply system is small and is neglected in the model.

## **3 Optimization of Operating Conditions**

### ***3.1 Optimization Model***

The fuel cell stack delivers electricity at high efficiency. However, the operation of the on-board auxiliaries significantly affects the performance and efficiency of fuel cell system. The fuel cell system optimization model was first developed by the UCD fuel cell vehicle modeling group in 2002 to analyze various air supply configurations and



their tradeoffs and to search for the optimum operating conditions to maximize the net system power and system efficiency. The optimization model in this paper was developed based on the former model with additional consideration given to the flow field channel design in the fuel cell stack, sizing of the air supply system, and the impact of the humidification and oxygen consumption on the pressure loss.

The GUI of the quasi-steady fuel cell system optimization model is shown in Fig.4. The interface gives some key factors which affect the system optimization results. The fuel cell performance is sensitive to the mass flow of the reactants, which depends on the fuel cell stack design. The following are the key parameters: the number of cells, the active area of the cell, and flow field design including the channel shape, dimensions and spacing. In this optimization model, only rectangular flow channels are considered. A Vairex twinscrew compressor of 17.2 kW and a Solectria Induction motor and controller combination of 21 kW are employed for scaling the air supply system in the optimization model. Usually a compressor has best efficiency around the nominal operating point and lower efficiency in the lower load range. The ratio of compressor power to the maximum stack power is introduced to scale the air compression system.

Temperature, relative humidity, operating pressure and the air mass flow are the four key external variables that have a major impact on the performance of the fuel cell stack.

Assuming the stack temperature and the relative humidity are well controlled, the operating pressure and the air mass flow will determine the oxygen partial pressure at the cathode catalyst layer, which determines the resultant cathode overpotential for stack

current. In the optimization model, the average pressure in the stack is used to calculate the effect of the water vapor on the mass flow rate. Thermal and water management for fuel cells are challenging issues in automotive applications. Fuel cell operation at relatively low temperature requires a large radiator. A condenser is needed for recovering water for humidifying the inlet reactant gases. The losses from the coolant pump, radiator fan and condenser are small compared to the loss from the air compression subsystem. The water and thermal management components are scaled based results in [6] and the maximum stack power.

The saturated water vapor pressure is the function of only temperature and is 0.46733 atm. at 80 °C. The change of the air mass flow caused by humidification is significant and should be considered for calculating the pressure drop on the flow channels of the stack. The dry air mass flow in the stack decreases due to the oxygen consumption in electrochemical reaction. The effect of the consumed oxygen on the change of the dry air mass flow should not be neglected when the stoich. ratio (SR) is less than 2.0. The oxygen, nitrogen and hydrogen diffusion through the membrane is small and its impact on the mass flow is neglected. The mole mass of the exhaust dry air depends on SR. However, the effect of the oxygen consumption at the cathode on the air mole mass is less than 2 percent and can be neglected in the fuel cell system optimization model when the SR is less than 2. The vapor mass flow contributes significantly on the stack pressure loss and is related to the dry air mass flow, pressure drop, and the back pressure according to the ideal gas law. The average pressure in the stack is used to calculate the

water vapor mass flow. The average mass flow in the stack is used to calculate the pressure loss in the optimization model.

The actual pressure drop across the stack is related to the humid air mass flow, stack back pressure, and channel flow field plate design. The pressure loss can be obtained using the Darcy-Weisbach Law. In the optimization model, the maximum allowable pressure drop across the stack and the assumed flow path number (channel number) are known. First, the humid air flow rate is calculated with the back pressure, the dry air mass flow rate, and the interpolated pressure drop from the maximum allowable pressure drop. The actual pressure drop across the stack is then calculated. The model calculates for every triplet (the current density,  $J$ , the dry air mass flow,  $\dot{m}$  and the back pressure,  $P_r$ ) the net output power of  $P_{net}(J, \dot{m}, P_r)$ . Then it scans among those which have  $P_{net}(J, \dot{m}, P_r) > 0$  and are within the safe operational region of the compressor, to find the one with  $\max(P_{net}(J, \dot{m}, P_r))$ .

$$P_{net}(J, \dot{m}_{optimal}, P_{r,optimal}) = \max[P_{net}(J, \dot{m}, P_r)]$$

In other words, the optimal mass flow  $\dot{m}_{optimal}$  and back pressure  $P_{r,optimal}$  will yield the maximum net power for certain  $J$  values.

In the last part of the calculation, the maximum actual pressure drop is obtained from the optimal results and compared with the input allowable pressure drop. If the maximum actual pressure drop on the stack matches the allowable pressure drop, the selected channel number is acceptable and the optimum operating conditions are also acceptable. Otherwise, the channel number is varied and the model is run until the maximum

optimum pressure drop on the stack is acceptable (less than the allowable pressure drop). The optimization process is given in Fig.5.

### **3.2 Optimum Operating Conditions**

The number of cells in the stack is determined by the required voltage. The active cell area is obtained from the current needed at maximum power. The width/length ratio of a cell can be varied without changing the cell power at a given voltage. The channel dimensions are given according to the MEA mechanical properties. For optimal operation with varying SR and back pressure, the maximum allowable pressure drop across the stack is set to 0.4 atm. The flow path number (number of channels) is related to the maximum pressure drop in the cell. An initial channel number is assumed. The channel number is adjusted until the pressure drop for optimal operation approaches the allowable pressure drop. In the following analysis the relative humidity in the stack is set to 1.0 and the stack temperature is 80°C.

It is of interest to compare fixed and varying pressure operation of the system. Hence the optimization model was modified to optimize the SR for fixed back pressure operation. For that analysis, the channel number from the optimum case with varying SR and back pressure is used and the allowable pressure drop is adjusted to match the maximum actual pressure drop in the stack. The modified optimization model was run with fixed back pressures of 2.0, 1.5, and 1.1 atm. The simulation parameters are listed in Table 1. A plot of system efficiency vs. system net power is shown in Fig. 6. The optimal polarization

curves, the compressor responses, and the pressure drop across the stack for different operating modes are shown in Fig.7, Fig.8 and Fig.9, respectively.

The comparisons of the results for the different operating modes indicate the following:

- The fuel cell system with optimal varying back pressure can achieve higher system efficiency over the full load range (Fig.6) and can produce more power than the fuel cell system operating at constant back pressures.
- For the same fuel cell system with different operating modes, lower constant back pressure operation has higher pressure drop across the stack than other operating modes due to higher ratio of water vapor partial pressure to dry air partial pressure (Fig.9).
- At low power demand, the fuel cell system operating at low pressure and at optimal back pressure has higher system efficiency than the fuel cell system operating at high pressure because of relatively low parasitic losses.
- At high power demand, the high pressure operating mode and the optimal varying back pressure operation mode can achieve higher system efficiency compared to the low pressure operation due to the high oxygen partial pressure at the catalyst layer and low pressure loss on the stack.
- At medium load demand, there is no apparent difference in the system efficiency for the different operation modes. However, low pressure operation requires a much larger humidifier than high pressure operation.
- The optimal operation can achieve higher efficiency over wide load change. However, coordinated control of the compressor and the back pressure valve can be complicated

and is needed to avoid large transient voltage drops during rapid changes in power demand.

## 4 Simulation Results for Fuel Cell Vehicles

The optimum model of fuel cell operation was applied to the load-following DHFC vehicle [8] with an updated traction motor controller and a scalable dynamic fuel cell system model. The simulation results shown in Fig.10 indicate that the speed of the vehicle operating at the optimum conditions follows the drive profile seamlessly. However, the vehicle model with the dynamic fuel cell system has high voltage fluctuations. The high voltage drops that occur during fast accelerations can be avoided by hybridization of a fuel cell system with electric energy storage (batteries or ultracapacitors). Fig.11 shows the fuel cell system performance in a DHFC vehicle on the FUDS cycle. The system performance with the original quasi-steady fuel cell model [22] is also shown in Fig.11. It can be seen that the maximum power required during the FUDS drive cycle was approximated 40 kW. Most of the time the vehicle operates in low power range. Note that the fuel cell system efficiencies from the original quasi-steady and the new transient dynamic fuel cell vehicle calculations are consistent.

The fuel economy of fuel cell vehicles on various drive cycles was calculated using the new fuel cell system model. The vehicle and fuel cell system parameters used in the calculations are given in Table 2 (Case 1) and Table 3 (Case 2). The DHFC vehicle model with the fuel cell system operating at the optimum operating conditions was compared with the DHFC vehicle with the fuel cell system operating at the fixed back pressures of 2.0 atm., 1.5 atm. and 1.1 atm. The fuel economies (Fig.12) for the various

driving cycles indicate that optimal varying back pressure operation can achieve a higher vehicle fuel economy compared to fixed high back pressure operation. The vehicle with the fuel cell system operating at the fixed low pressure has almost the same fuel economy as that of the vehicle with optimal varying back pressure operation. However, the low constant back pressure operation has lower maximum net fuel cell output power which will affect the vehicle acceleration performance. The low back pressure operation needs a larger humidifier and creates a higher stack pressure drop.

Simulations were also run for the DHFC vehicle with a smaller fuel cell system (Case 2) to assess the effect of the size of the fuel cell system on vehicle fuel economy. The vehicle and fuel cell system parameters are given in Table 3. The simulated vehicle fuel economies for the various driving cycles are presented in Fig.13. The vehicle fuel economy in Fig.13 (case 2) was normalized with respect to the corresponding fuel economy of Case 1 for the each drive cycle and plotted in Fig. 14. It can be seen that employing a smaller fuel cell system in a DHFC vehicle has a little impact on the vehicle fuel economy for the optimal varying back pressure operation and low back pressure operation, but can significantly improve the fuel economy for the fixed high back pressure operation.

## 5 Conclusions and Discussion

A scalable fuel cell system model was developed for optimizing the operation of the fuel cell system. The design parameters of the stack and the sizing of the air supply and the water and thermal management subsystems were selected to maximize the system efficiency. The conditions for different operating modes were optimized by using the

system optimization model. The effects of optimizing the fuel cell system operation and the sizing of the fuel cell system on the vehicle fuel economy were studied for various drive cycles for a load following direct hydrogen fuel cell vehicle using the new transient dynamic fuel cell system model.

The results of the study are summarized below:

- Compared to fixed back pressure operation, the fuel cell system with the optimal varying back pressure operation can achieve higher system efficiency over the full operating range and can maximize the net system power.
- For optimal varying back pressure operation and fixed low back pressure operation, the size of the fuel cell system has a little effect on the fuel economy of the vehicle. However, reducing the size of the fuel cell system will benefit the fuel economy of a DHFC vehicle with a fuel cell system operating at the fixed high back pressure.
- The vehicle with the fuel cell system operating at fixed low pressure has almost the same fuel economy as that of the vehicle with optimal varying back pressure operation. However, the low constant back pressure operation has lower maximum net output power which will affect the vehicle acceleration performance. The low back pressure operation needs a larger humidifier and creates a higher pressure drop across the stack.

The optimal operation of fuel cell system varies the back pressure and air supply SR according to the change of the power demand. These rapid changes in the operating conditions of the fuel cell stack can have a major impact on the lifetime of the fuel cell



stack due to the mechanical stresses on the MEA and the stack accessory components. Coordinative control of the mass flow and pressure of the cathode and anode sides of the stack is required. This is the main drawback of the optimal operation of the fuel cell system for automotive applications. These variations in operating conditions can be reduced by hybridizing the fuel cell system by the addition of electrical energy storage with batteries or ultracapacitors. In addition to reducing the sudden changes in operating conditions, the energy storage permits the capture of regenerative braking energy, which should improve the fuel economy by 10-15%. The fuel cell – battery hybrid vehicle and its control strategy and the effect of the transient response of the fuel cell system on the hybridization will be addressed in the future work.

## Acknowledgements

The work presented in this paper was supported by the STEPS and PHEV programs of the Institute of Transportation Studies of the University of California, Davis. This research is based on the previous research of the FCVMP team. Please refer to <http://www.its.ucdavis.edu> for further details about the STEP and PHEV programs, sponsors, and previous reports/papers.

## References

1. R.K. Ahluwalia, X. Wang, R. Kumar, Fuel Cell Systems for Transportation: Status and Trends, J. Power Sources, 177(1), 2008, pp.167-176.

2. T.E. Springer, T. A. Zawodzinski, S. Gottesfeld, Polymer Electrolyte Fuel Cell Model, *J. Electrochem. Soc.*, 138(8), 1991, pp. 2334-2342.
3. T.E. Springer, M. S. Wilson, S. Gottesfeld, Modeling and Experimental Diagnostics in Polymer Electrolyte Fuel Cells, *J. Electrochem. Soc.*, 140(12), 1993, pp. 3513-352.
4. D.M. Bernardi, M.W. Verbrugge, A Mathematical Model of the Solid-Polymer-Electrolyte Fuel Cell, *J. Electrochem. Soc.*, 139(9), 1992, pp. 2477-2491.
5. D.J. Friedman and R.M. Moore, PEM Fuel Cell System Optimization, Proceedings of the 2<sup>nd</sup> International Symposium on Proton Conducting Membrane Fuel Cells II, Electrochemical Society, Pennington, NJ, 1998, p. 407-423.
6. P. Badrinarayanan, A. Eggert, R.M. Moore, Minimizing the Water and Thermal Management Parasitic Loads in Fuel Cell Vehicles, *International Journal of Transport Phenomena*, 2001 3(3) 213-229.
7. J.M. Cunningham, M.A. Hoffman, A Comparison of High Pressure and Low Pressure Operation of PEM Fuel Cell Systems, SAE, Detroit MI, March 2001 (paper number 2001-01-0538).
8. D.J. Friedman, Maximizing Direct-Hydrogen Pem Fuel Cell Vehicle Efficiency-Is Hybridization Necessary? SAE 1999 (paper number 1999-01-0530).
9. D.J. Friedman, A. Eggert, P. Badrinarayanan, J.M. Cunningham, Balancing Stack, Air Supply, and Water/Thermal Management Demands for An Indirect Methanol Pem Fuel Cell System, SAE 2001, (paper number 2001-01-0535).
10. F. Barbir, M. Fuchs, A. Husar, J. Neutzler, Design and operational characteristics of automotive PEM fuel cell stacks, SAE 2000 (paper number 2000-01-0011).

11. J.M. Cunningham, M.A. Hoffman, R.M. Moore, D.J. Friedman, Requirements for a Flexible and Realistic Air Supply Model for Incorporation Into a Fuel Cell Vehicle (FCV) System Simulation, SAE 1999, (paper number 1999-01-2912).
12. J. Cunningham, R. Moore, S. Ramaswamy, K.-H. Hauer, A Comparison of Energy Use for a Direct-Hydrogen Hybrid Versus a Direct-Hydrogen, Load-Following Fuel Cell Vehicle, SAE 2003 (paper number 2003-01-0416).
13. S. Gelfi, A.G. Stefanopoulou, J.T. Pukrushpan, H. Peng, Dynamics of Low-Pressure and High-Pressure Fuel Cell Air Supply System, 2003 American Control Conference Denver, ACC2003, Colorado, 2003.
14. S. Pischinger, C. Schonfelder, J. Ogrzewalla, Analysis of dynamic requirements for fuel cell systems for vehicle applications, Journal of Power Sources, 154(2), 2006, pp. 420-427.
15. J.T. Pukrushpan, A.G. Stefanopoulou, H. Peng, Modeling and Control for PEM Fuel Cell Stack System, Proceedings of the American Control Conference, Anchorage AK, May 2002, pp.3117-3122.
16. J.T. Pukrushpan, H. Peng, A.G. Stefanopoulou, Simulation and Analysis of Transient Fuel Cell System Performance Based on a Dynamic Reactant Flow Model, Proceedings of IMECE' 02, 2002 ASME International Mechanical Engineering Congress & Exposition, Nov. 2002.
17. C.-J. Sjostedt, J.-G. Persson, The Design of Modular Dynamical Fluid Simulation Systems, OST, Stockholm Sweden, 2005.
18. J.T. Pukrushpan, A.G. Stefanopoulou, H. Peng, Control of Fuel Cell Power Systems, Springer, 2004.

19. J. Reuter, U.-J. Beister, N. Liu, D. Reuter, B. Eybergen, M. Radhamohan, A. Hutchenreuther, Control of a Fuel Cell Air Supply Module (ASM), SAE 2004 (paper number 2004-01-1009).
20. A. Miotti, A.D. Domenico, Y.G. Guezennec, S. Rajagopalan, Control-oriented model for an automotive PEM fuel cell system with imbedded 1+1D membrane water transport, Vehicle Power and Propulsion, 2005 IEEE Conference, Sept. 2005, pp. 611-618.
21. K.-H. Hauer, A. Eggert, R.M. Moore, S. Ramaswamy, The Hybridized Fuel Cell Vehicle Model of the University of California, Davis, SAE 2001, Detroit MI, March 5-8, 2001 (paper number 2001-01-0543).
22. R.M. Moore, K.H. Hauer, D. Friedman, J.M. Cunningham, P. Badrinarayanan, S. Ramaswamy, A. Eggert, A dynamic simulation tool for hydrogen fuel cell vehicles, Journal of Power Sources, 141(2) 2005, pp. 272-285.
23. J.M. Cunningham, R.M. Moore, S. Ramaswamy, A Comparison of Energy Use for a Direct-Hydrogen Hybrid versus a Direct-Hydrogen Load-Following Fuel Cell Vehicle, SAE 2003 (paper number 2003-01-0416).
24. H. Zhao, A.F. Burke, Modeling and Optimization of PEMFC Systems and its Application on Direct Hydrogen Fuel Cell Vehicles, 2008.

## Table of Figures

Fig. 1 Direct hydrogen fuel cell system Schematic Diagram

Fig. 2 Diagram of the fuel cell system for direct hydrogen fuel cell vehicles

Fig. 3 Driver end of the direct hydrogen fuel cell vehicle model

Fig. 4 Interface of the fuel cell system optimization model

Fig. 5 Flowchart of searching for the optimum operating conditions

Fig. 6 Comparison of the optimal system efficiency for different operating modes:  
optimal varying back pressure operation and fixed back pressure of 2.0, 1.5, and 1.1 atm.

Fig. 7 Optimal fuel cell polarization curves for different operating modes

Fig. 8 Optimal compressor quasi-steady responses for different operating modes

Fig. 9 Pressure drop across the stack vs. current density

Fig. 10 Simulation results of the DHFC vehicle with the dynamic fuel cell system model  
on the FUDS cycle

Fig. 11 Comparison of the system performance with the quasi-steady and transient  
dynamic fuel cell system model on the FUDS drive cycle

Fig. 12 Fuel economy of the DHFC vehicle operating at optimal back pressures and fixed  
back pressures of 2.0, 1.5, and 1.1 atm. on different driving cycles (Case 1)

Fig. 13 Fuel economy of the DHFC vehicle with a smaller fuel cell system operating at  
optimal back pressures and fixed back pressures of 2.0, 1.5, and 1.1 atm. on different  
driving cycles (Case 2)

Fig. 14 Normalized fuel economy of the DHFC vehicle (case 2) to the DHFC vehicle  
(case 1)

## Tables

Table 1 Fuel cell stack and system parameters

Table 2 Vehicle and fuel cell system parameters (Case 1)

Table 3 Vehicle and fuel cell system parameters (Case 2)



Fig. 2

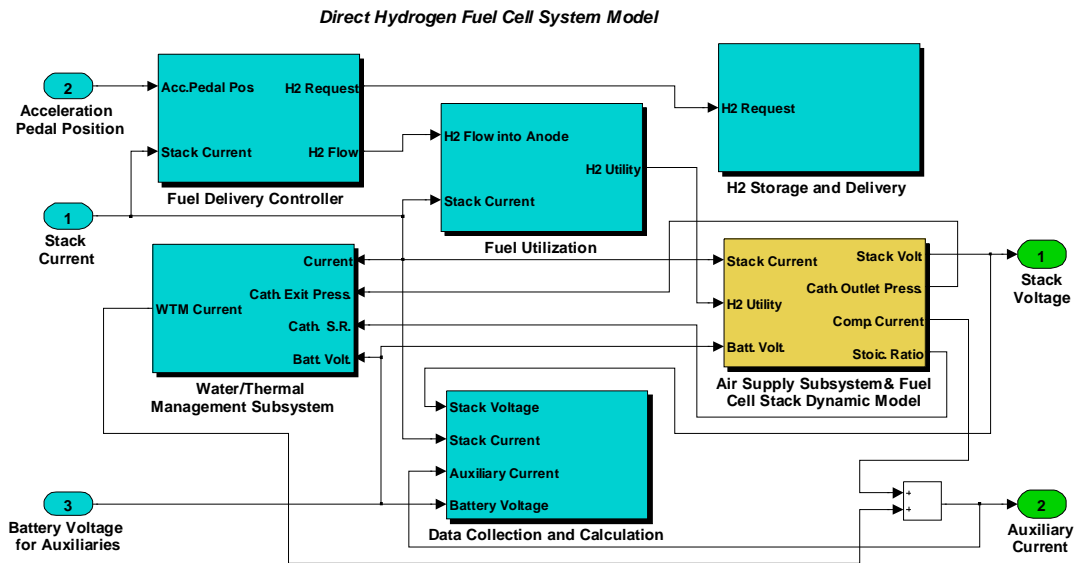




Fig. 3

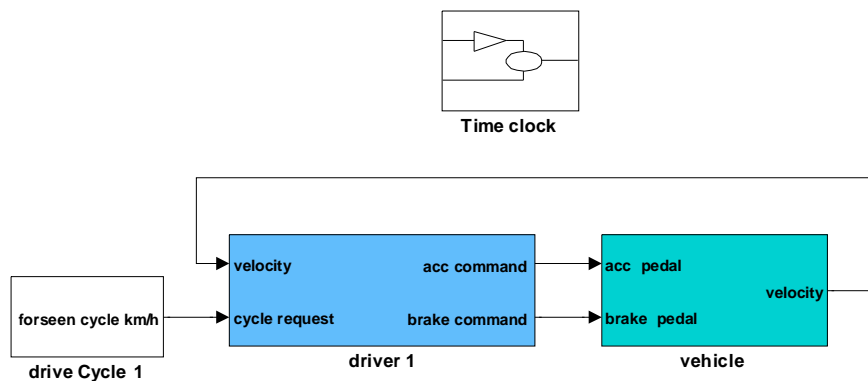


Fig. 4

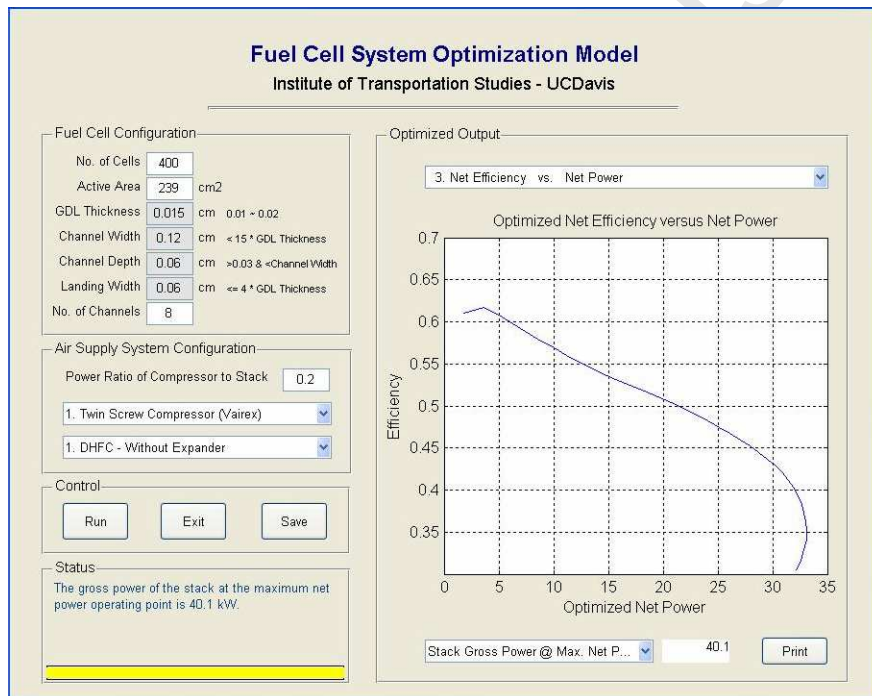


Fig. 5

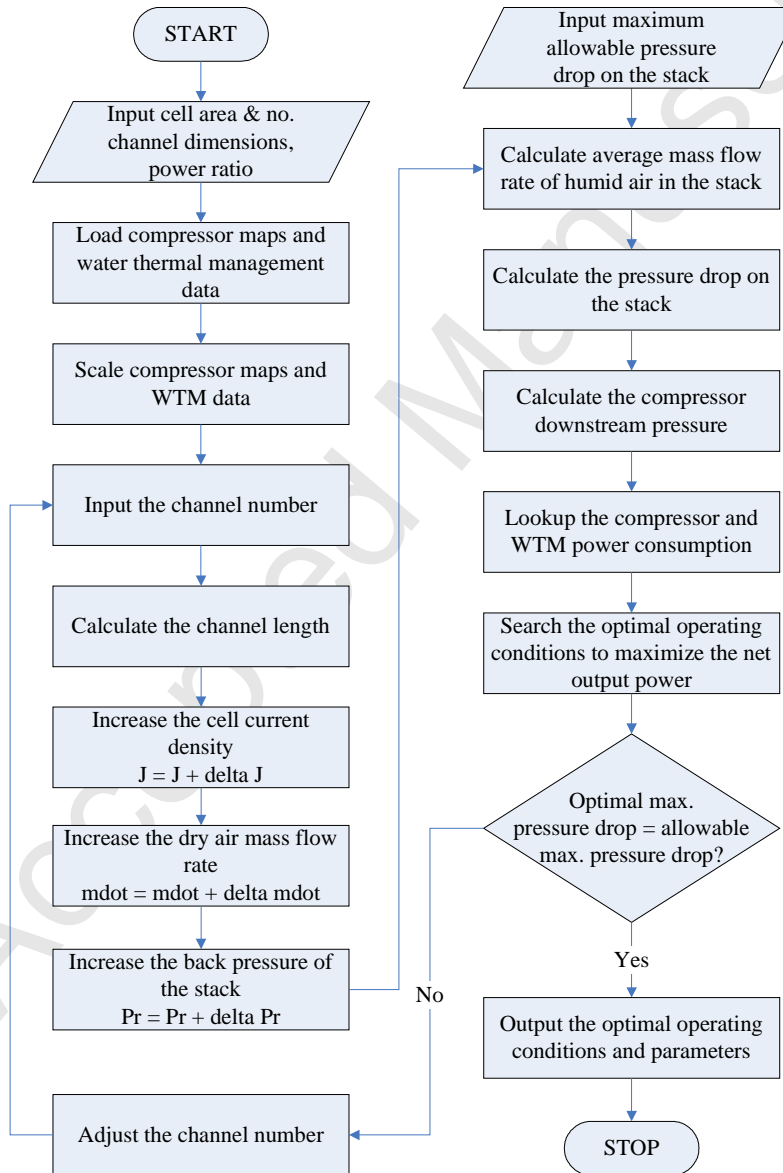


Fig. 6

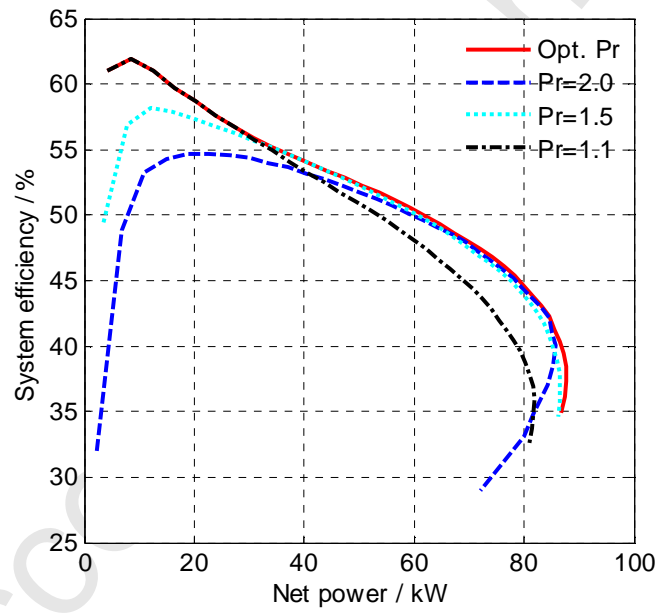


Fig. 7

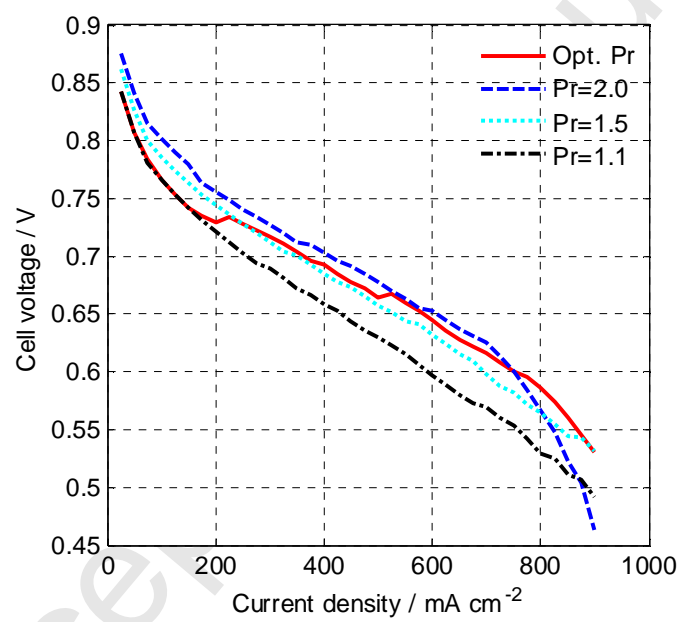


Fig. 8

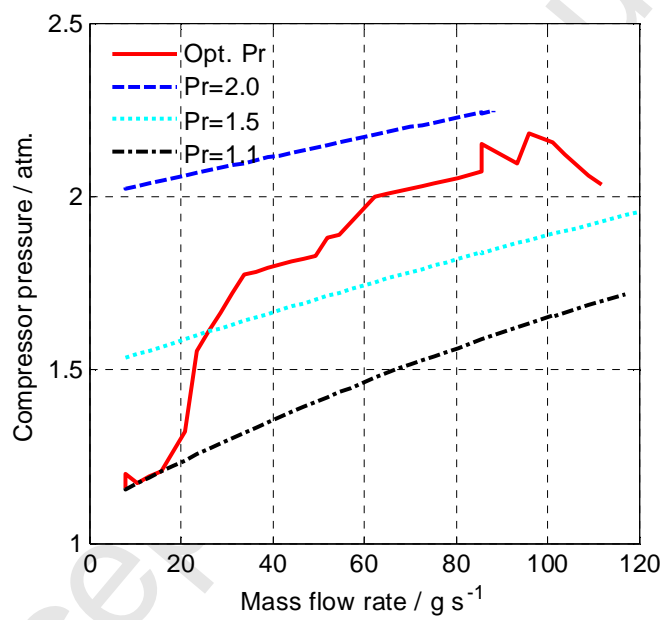


Fig. 9

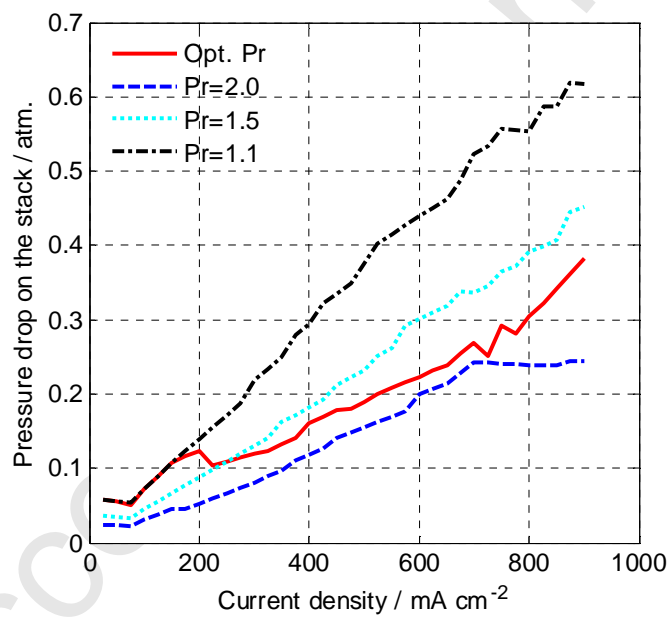


Fig. 10

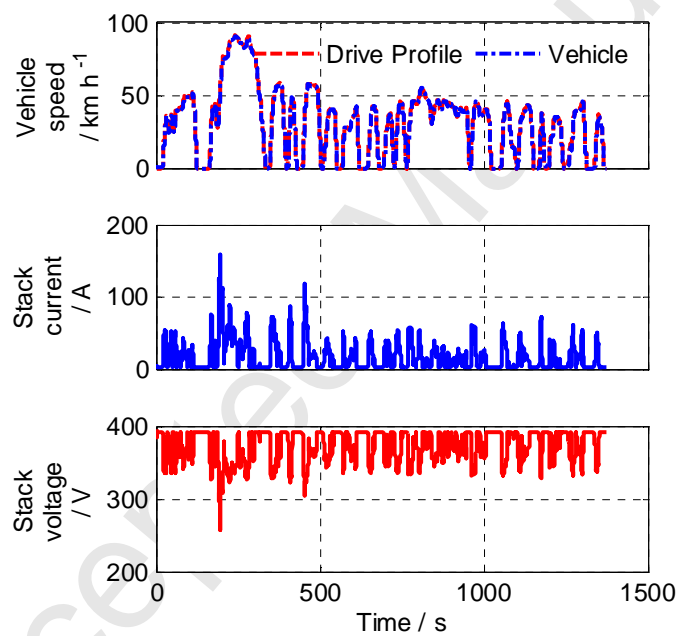




Fig. 11

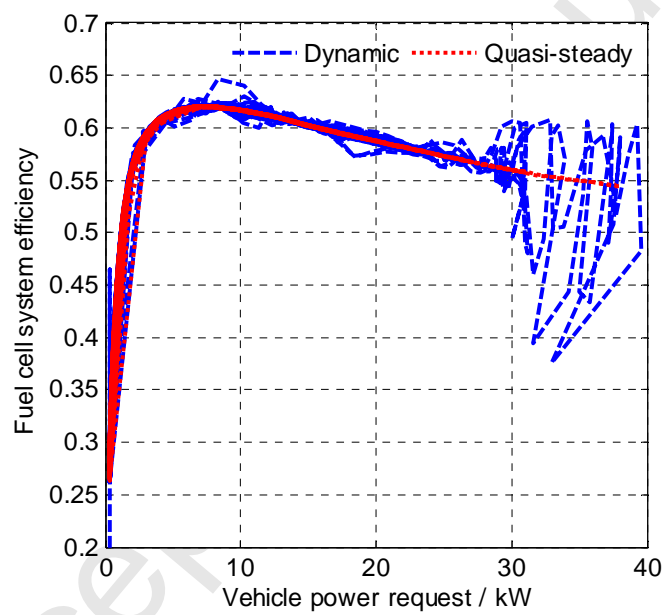


Fig. 12

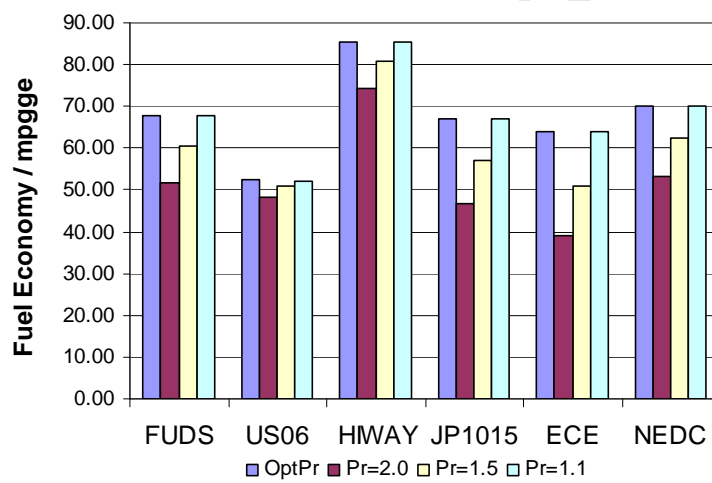


Fig. 13

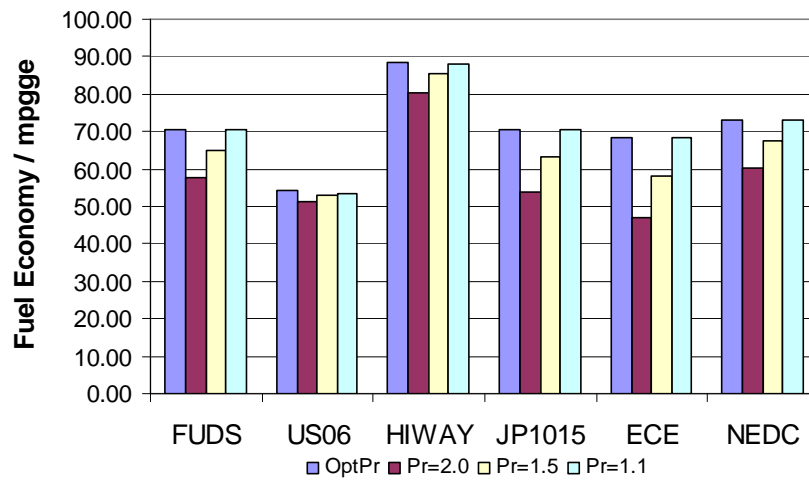


Fig. 14

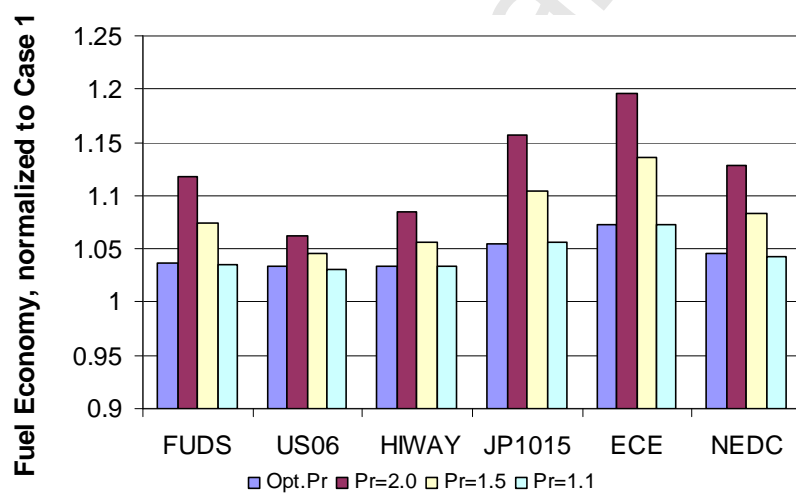


Table 1

## Fuel cell stack and system parameters

No. of Cells	440	Width of Flow Path (mm)	1.2
Active Area (cm <sup>2</sup> )	510	Depth of Flow Path (mm)	0.6
No. of Flow Paths	15	Width of Landing Area (mm)	0.6
Thickness of GDL (mm)	0.15	Power Ratio of Twin Screw Compressor to Stack	0.2

Table 2

Vehicle and fuel cell system parameters (Case 1)

Vehicle and System Parameters	
Drag Coefficient	0.3
Frontal Area (m <sup>2</sup> )	2.2
Vehicle Hotel Load (kW)	0.3
Vehicle Mass (kg)	1500.0
Electric Motor (kW)	75.0
Fuel Cell Stack and Auxiliaries	
Max. Net Power (kW)	87.6
Gross Power (kW)	106.2
Number of Cells	440
Cell Area (cm <sup>2</sup> )	510.0
Compressor (kW)	17.2

Table 3

Vehicle and fuel cell system parameters (Case 2)

Vehicle and System Parameters	
Drag Coefficient	0.3
Frontal Area (m <sup>2</sup> )	2.2
Vehicle Hotel Load (kW)	0.3
Vehicle Mass (kg)	1500.0
Electric Motor (kW)	50.0
Fuel Cell Stack and Auxiliaries	
Max. Net Power (kW)	58.4
Gross Power (kW)	70.8
Number of Cells	440
Cell Area (cm <sup>2</sup> )	340
Compressor (kW)	11.4